

3D EXPERIMENTAL DATA ANALYSIS OF DIRECT AND INVERSE PROBLEM USING MULTIFREQUENCY AND EMAT APPROACH FOR CRACK DETECTION IN PLATE STRUCTURE

Mohammed CHEBOUT

L2ADI Laboratory, Department of electrical engineering, Djelfa University, Algeria
chebout_med@yahoo.fr

Mohammed Rachid MEKIDECHE

L2EI Laboratory, Department of electrical engineering, Jijel, University, Algeria
mek_moh@yahoo.fr

Abstract: *The analysis of information, resulting from eddy currents nondestructive testing method proves very interesting, for the detection and identification of defects in many different industrial structures. We review in this paper, a three dimensional numerical approach based on AV-A formulation in order to determine interaction of induced eddy currents in the metal test specimen with flaws, and the coupling of these interaction effects with the moving test probe. In this paper, experimental and theoretical results are illustrated of three dimensional planar crack defect modeling, located in Benchmark metal plate structure by analyzing change in impedance of an absolute coil probe using multifrequency and electromagnetic acoustic transducer (EMAT) technique. An evaluation material characterization using neural network optimization technique is done*

Key words: *Eddy current, crack, nondestructive evaluation, Multifrequency and EMAT techniques, Neural network*

1. Introduction

In practice, the experts of nondestructive testing NDT in charge of inspection have problems of test results interpretation, against established criteria in conjunction with the designer. It is a question of qualifying, not necessary quantifying product status without alteration of its characteristics in order to allow for defects that could affect their behavior in service [1]. Since the techniques do not alter the product being inspected, they are valuable methods for material and component evaluation, troubleshooting and research that can save both money and time [2]. The most commonly used NDE techniques in industry, including visual inspection (VI) [3-4], radiography technique (RT) [5], ultrasonic technique (UT) [6], magnetic flux leakage (MFL) [7], thermography method (TM)[8], and eddy current technique (ECT) [9] which is well suited to such applications since it is easy to implement, sensitive, robust and eco-aware.

The principle of eddy current nondestructive testing (ECNDT) is based on the generation of eddy currents in the conductive material, by means of an alternative source and generating a variable magnetic field that interacts with the materials under test. Changes in electrical conductivity or magnetic permeability of the test object, or the presence of crack defects, will cause an eddy current change and a corresponding change in the phase and amplitude of the measured current is detected. In industrial plants and under certain conditions, this technique allows revealed crack defects effectively in the conductive structure and gives accurate results [2-9].

Eddy current nondestructive testing can be used for a variety of applications. One is to detect defect and inspect the condition of samples which may be related to the surface-cracks, sub-surface flaw and degradation. For this kind of application, the nature of the crack defect must be well understood in order to obtain good inspection results. Another important application of eddy current testing is to measure the properties of materials, including the electrical conductivity, magnetic permeability. Therefore, eddy current measurements can be used to sort conductive materials (metal has different conductivity) and to characterize heat and stress treatment, which normally lowers the conductivity [10]. It can be also used to measure the thickness of thin materials, which vary from millimeters, to achieve the micrometers for highly sensitive industrial applications.

According to the operating mode of eddy current control, there are two types of eddy current probe: Absolute and differential probe coil. The first one measures signals changes received relative to itself, while the second compares the result from the two probes coil. The complexity of the operation is relative depending on the probe parameters and the nature of the device under test

More information can be extracted, according to operating mode as measurement of the electrical conductivity and magnetic permeability, thickness measurement, the determination of the target distance-sensor effect (Lift-off)...etc. Differential probes have high common mode rejection. They are therefore sensitive to sudden changes such as cracks, voids, and edges, in part because the signal is not masked by responses from slowly varying changes [11]. Absolute probes, on the other hand, are sensitive not only to sudden changes (such as discontinuities), but also to slowly varying geometry and material properties.

2. Mathematical model

ECNDT is a technique that is based on the theory of electromagnetic fields. The analysis and the mathematical model, for calculating these induced currents in the steam generator tubes, is done using electromagnetism laws as basis, including Maxwell equations quasistatic approximations.

A number of approaches already exist to model the interaction between the probe and the tested structure. The most general ones in complex geometries use the numerical methods. Modeling and simulation of eddy currents testing provide a good basis for allowing an early evaluation of part inspection. Several numerical formulations based on the finite element method have been proposed to overcome the well-known difficulties related to this kind of this open boundary problem both differential and integral [12]. Among the differential formulations we recall the H- Φ formulation proposed by Bossavit and Verite [13], the T- Ω formulation discussed by Carpenter [14], later by Brown [15] and Albanese and Rubinacci [16], the A-V formulation proposed by Biro [17]. The main advantage of the differential formulation is that the matrices of the solving system are sparse, and this is quite very important for the computational cost.

In this paper, we apply a three dimensional FE method for calculating eddy current probe signals due to cracks in order to characterize material proprieties. The set of equations governing the behavior of multiphysics systems, variables in time, can be expressed from Maxwell equations as follows:

$$\nabla \times (\mu^{-1} \nabla \times \mathbf{A}) + j\omega\sigma\mathbf{A} + \sigma\nabla V = 0 \quad (1)$$

$$\nabla \cdot \sigma(j\omega\mathbf{A} + \nabla V) = 0 \quad (2)$$

$$\nabla \times (\mu^{-1} \nabla \times \mathbf{A}) = \mathbf{J} \quad \text{Nonconducting regions} \quad (3)$$

Using Galerkin techniques, the Dirichlet boundary conditions require nodal potentials to be set to the known values [18-20].

Regarding the standard Neumann conditions, they can be considered in a natural way. In our case, where the use of magnetic vector potential and electric scalar potential, we consider the Galerkin weak form illustrated by the expressions (1) and (2), with $\bar{\Psi}$ and Ψ denoting the weighting functions which coincide with the shape functions in a finite element realization [21]. Then (1) and (2) are replaced by:

$$\int_{\Gamma} \bar{\Psi} \cdot \nabla \times (\mu^{-1} \nabla \times \bar{\mathbf{A}}) d\Gamma + \int_{\Gamma} j\omega\sigma \bar{\mathbf{A}} \bar{\Psi} d\Gamma + \sigma \bar{\Psi} \int_{\Gamma} \nabla V d\Gamma = 0 \quad (4)$$

$$\int_{\Gamma} \Psi \nabla \cdot \sigma (j\omega \bar{\mathbf{A}} + \nabla V) d\Gamma = 0 \quad (5)$$

The components of impedance are given as follows:
 $R = P / I^2$ and $L = 2W / I^2$ (6)

In this case the unknown parameters P and W can be respectively expressed by:

$$P = \int_{\Gamma} \mathbf{J} \mathbf{E}^* d\Gamma \quad \text{and} \quad W = \frac{1}{2} \int_{\Gamma} \mathbf{H} \mathbf{B}^* d\Gamma \quad (7)$$

Here, $\vec{E} = -\nabla V - j\omega \vec{A}$, $\vec{B} = \nabla \times \vec{A}$ and $\vec{H} = \vec{B} / \mu$ (8)

3. Application and results

In figure 1, the schematic configuration of the analysis model is shown, and in Table 1 a geometrical and physical model parameters are specified. The finite element mesh showing in contains 79162 nodes and 1021837 tetrahedral elements. A preconditioning technique, called the symmetric successive over-relaxation (SSOR) method is employed to minimize computation time and memory.

The pancake type absolute circular air-cored coil probe is scanned, parallel to the x-axis, along the length of a plane Benchmark structure containing rectangular crack shown in figure 1.

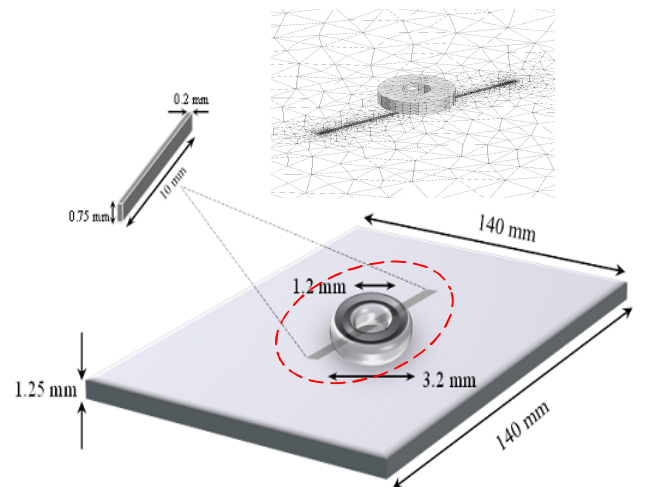


Fig. 1. Geometrical model with crack shape illustration

Table 1. Geometrical and physical parameters

Parameter	Plate thickness	Plate length	Plate width
Value [mm]	1.25	140	140
Parameter	Crack width	Crack length	Crack depth
Value [mm]	0.20	10.0	0.75
Parameter	Coil inner radius	Coil outer radius	Coil height
Value [mm]	0.60	1.60	0.80
Parameter	Conductivity [MS/m]	Lift-off	Frequency [kHz]
Value [mm]	1.00	0.50	150 & 300

We illustrate in figure 2, induced eddy current density cartography. The crack defect is not present here but we can remark effect of bobbin coil on this parameter. Under the given frequency and coil lift-off, the impedance is calculated as function of coil position [22]. The impedance change represented by the resistance and reactance components in figure 3 is evaluated as function as coil position for two frequencies values 150 kHz and 300 kHz. Our calculus and numerical results are compared with experimental one and we remark a good agreement between us.

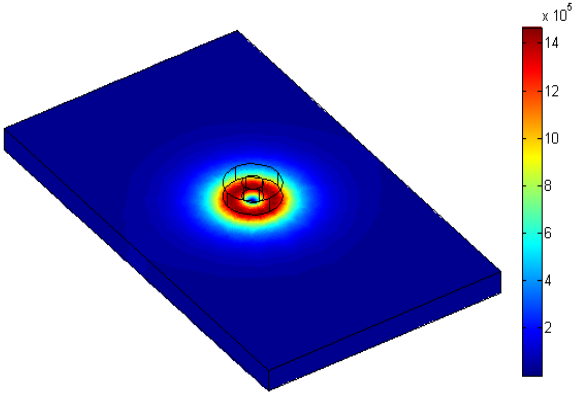


Fig.2 Eddy current distribution without defect

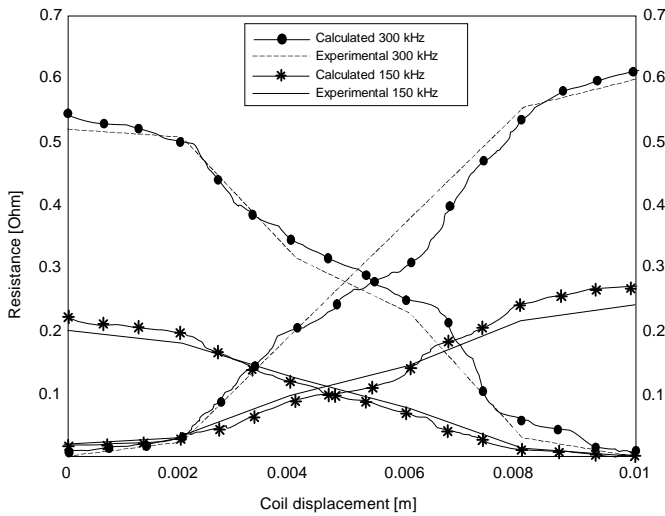


Fig.3 Experimental and numerical results of impedance components vs coil displacement

The coil impedance $Z = R + jX$ is the typical of eddy current distribution in the material. In order to eliminate the influence of the electrical proprieties of the coil itself, the normalized impedance has been calculated [23]

$$R_n = (R - R_0) / R_0 \quad (9)$$

$$X_n = X / X_0 \quad (10)$$

Where R_n is the normalized resistive component, and X_n represent the normalized reactive component.

The normalized impedance analysis is widely preferred for the analysis of eddy current signals in a complex-plane diagram. It is defined as the ratio of the measurement coil impedance due to the presence of the test object and the coil impedance as measured in the air, which provides the relative magnitude of eddy current signal with regards to background measurement. We illustrate in figure 4, normalized impedance plane diagrams which consist to plot the real part as functions as imaginary part of normalized impedance for seventeen values of frequency distributed between 500 Hz and 5MH. We observe in this figure, an excellent concordance between experimental result and finite element approach.

In order to evaluate the limits of flaw detection, we considered the notion of ΔR_n and ΔX_n [24].

$$\Delta R_n = R_n(\text{Unflawed}) - R_n(\text{flawed}) \quad (11)$$

$$\Delta X_n = X_n(\text{Unflawed}) - X_n(\text{flawed}) \quad (12)$$

We plot variation in normalized impedance components for four depth defect values: at benchmark surface, at 0.05 mm, 0.10 mm and at 0.15 mm from a plate surface as shown in figure 5 and figure 6 which describe variation in real part and imaginary part of normalized impedance respectively.

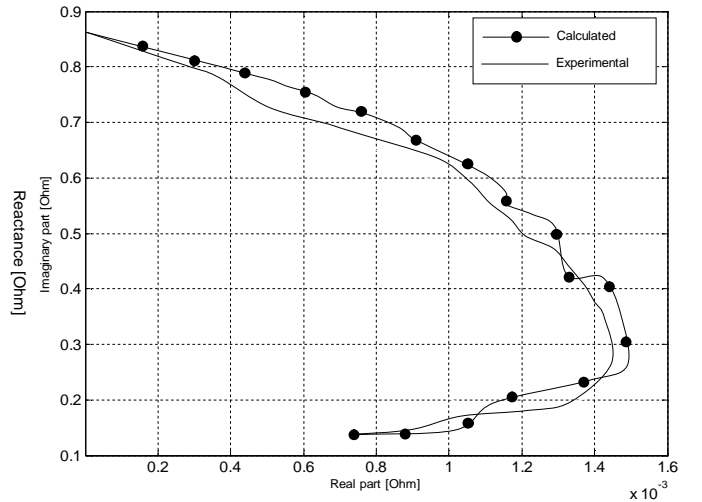


Fig.4 Experimental and calculated results of normalized impedance plane diagram

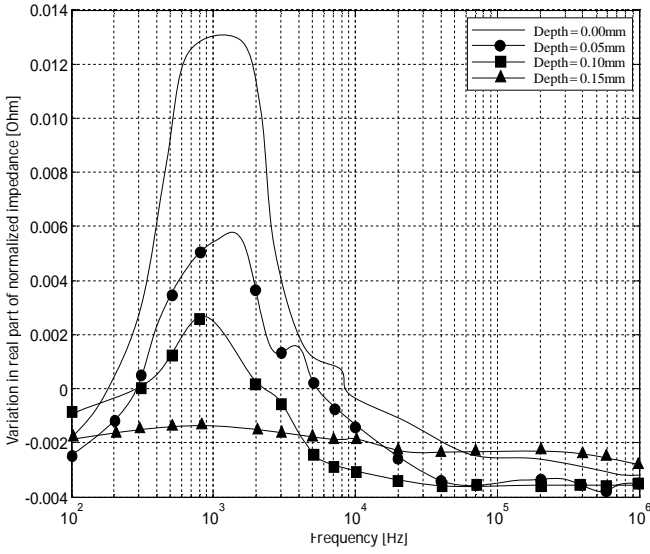


Fig.5 ΔR_n vs frequency for different depth crack

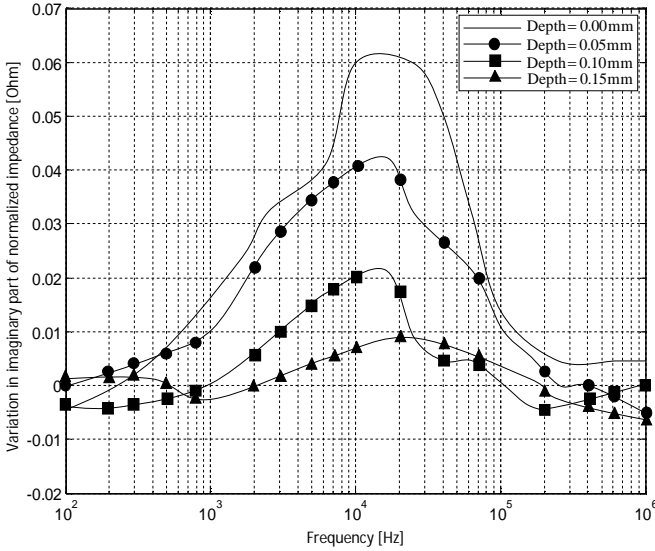


Fig.6 ΔX_n vs frequency for different depth crack

The effectiveness of eddy current testing using Multifrequency technique is limited by skin effect to only thin and nonmagnetic structural parts [25]. We use in this second part of this paper, pulsed eddy current technique which used to measure coating thickness, inspect hidden corrosion and inspect cracks in metal [26]. The depths of cracks are 0.5, 0.8, and 1mm from the top of the metal as shown in figure 7. We assumed that the thickness of the samples is much bigger than the eddy current diffusion depth. The electromagnetic field will not penetrate the metal. The current difference for metal with crack and same metal without crack was recorded. Figure 8 shows the PEC signals of fatigue cracks on Al sample. The results show that the measured signals on Al sample are very strong. Deeper cracks exhibit stronger signals.

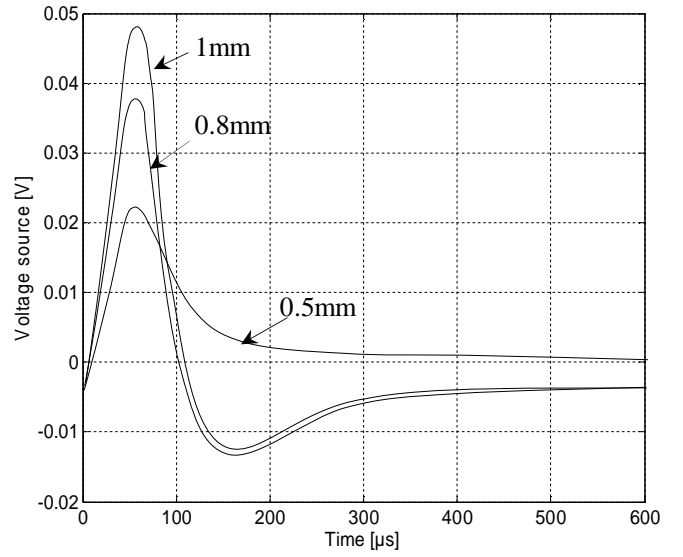


Fig.7 Pulsed eddy current signals of different deep crack

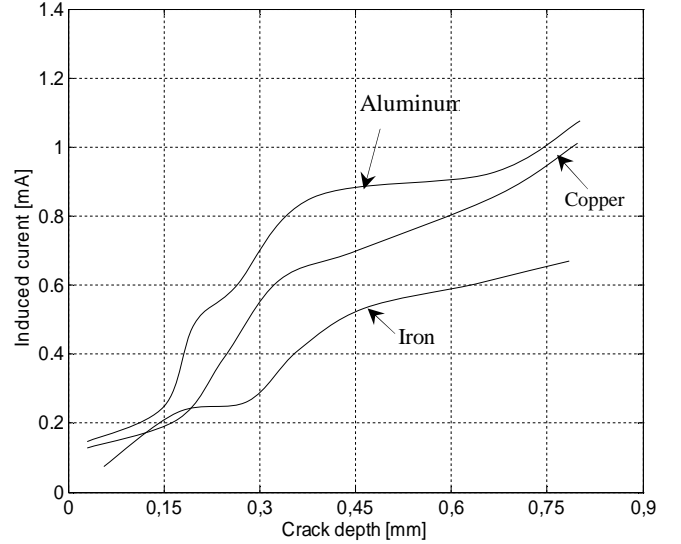


Fig.8 Induced Current vs crack depth

Nevertheless, the relationship between the peak PEC signals and crack depth can't be explained using the electromagnetic diffusion rule.

4. Inverse problem

The increasing interest to the neural network can be explained by their successful implementation in different areas [27]. These methods are also widely used in eddy current non-destructive evaluation. Multilayer perceptrons (MLPs), also referred as multi-layer feed forward neural networks, comprise an input layer, one or more hidden layer, and an output layer. Using this approach, the solution from the artificial neural network of an inverse problem is to estimate unknown weights or parameters from a set of input-output examples during learning [28].

Parameters identification using neural network can be recast as a problem in multidimensional interpolation, which consists of finding the unknown nonlinear relationship between inputs and outputs in a space spanned by the activation functions associated with the neural network nodes such as shown in Figure 9.

Learning in a MLP is an unconstrained optimization problem, which is subject to the minimization of a global error function depending on the synaptic weights of the network. For a given training data consists of input-output patterns, values of synaptic weights in a MLP are iteratively updated by a learning algorithm to approximate the target behavior. This update process is usually performed by back-propagating the error signal layer by layer and adapting synaptic weights with respect to the magnitude of error signal [29-31]. The input space corresponds to the signal generated by sensors and the output corresponds to the electromagnetic parameters such as relative magnetic permeability and electrical conductivity. The neurons in the hidden layer and the examples in the training set have the same number and the values of the widths of the Gaussian functions are identical for all the neurons of the hidden layer.

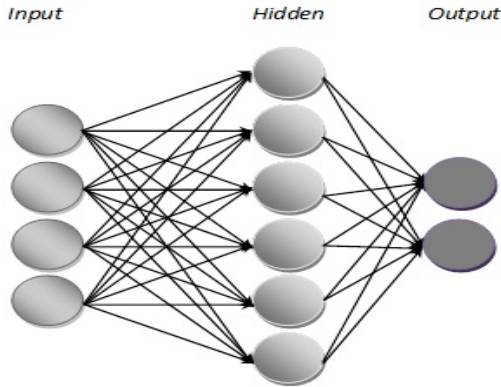


Fig.9. Multilayer perceptrons neural network

The adjustment of internal parameters of the MLP neural networks is performed by minimizing the mean square error (MSE) which is used as a cost function, and measured between the output of the network and the desired solution when the corresponding inputs are presented to the NN [31]. In this case the mean square error value is computed as variation in impedance values showing follows:

$$f = \sum_{i=1}^n \left| \Delta Z^i - \Delta Z_{meas}^i \right|^2 \quad (13)$$

If the agreement is unsatisfactory, the updated and a new prediction are made. The process is busy through a number of iterations until predictions and observations match to within a reasonable tolerance.

Figure 10 shows the evolution of the MSE on training set and validation and test sets according to the width in the impedance measurements. The optimal value of the width is 62 neurons

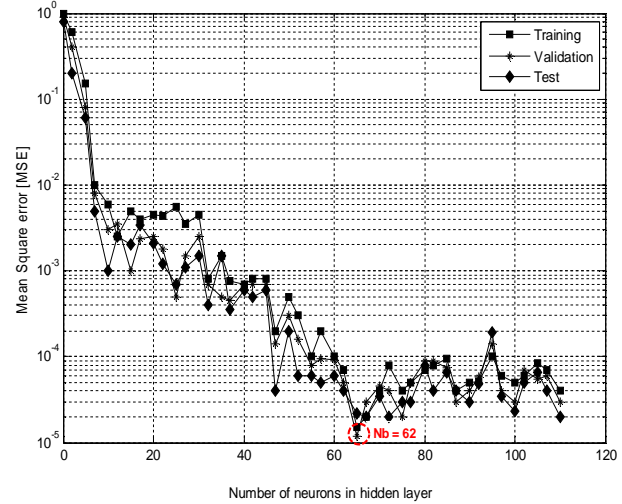


Fig.10. MSE error evolution vs Nb of neurons

5. Conclusion

Multifrequency and Pulsed eddy current technique applied on inspecting metal surface cracks from theoretical and experimental aspects will be demonstrated in this paper. The impact of various frequencies values, peak pulsed eddy current signal amplitude and crack depth parameters on signals response is investigated by numerical way using three dimensional finite element model. Theoretical results supported by experiments have confirmed the accuracy of the proposed model. Another effective approach based on MLP neural network is introduced in order to evaluate and characterize conductive material. The results obtained here are significant. Further work of the authors will concern reconstruction of crack shapes by adopting an advanced procedure for diagnosis of real cracks profiles from simulated eddy current testing response signals followed by experimental verifications if possible.

References

1. Janousek, L., Smetana, M., and Alman, M., : *Decline in ambiguity of partially conductive cracks depth evaluation from eddy current testing signals*, Intl. J. Appl. Electr.Mech.,(2012),No.39,p. 329-334
2. Pasadas,D., Rocha,T., Ramos,H.G., and Ribeiro,A.L., : *Evaluation of portable ECT instruments with positioning capability*, Measurement, (2012),No.45, p 393-404.
3. Malhotra,V.M., Carino,N.J., *Handbook on Nondestructive Testing of Concrete*, CRC Press Inc, USA, 2004

4. Bray,D., Stanley,R.K.,: *Nondestructive Evaluation : A Tool in Design, Manufacturing and Service*, CRC Press Inc, USA, 1997
5. Alaknanda,R.S., Kumar,P.,: *Flaw detection in radiographic weldment images using morphological watershed segmentation technique*, NDT&E., (2009), No.42, p 2-8
6. Ramadas, S.N., Jackson, J.C., Tweedie, A., O'Leary,R.L., and Gachagan,A.,: *Conformally mapped 2D ultrasonic array structure for NDT imaging application*, Proceedings of IEEE Ultrasonics Symposium, 2010, p 33-36
7. Borsutzki,M., Kroos,J., Reimche,W., and Schneider,E.,: *Magnetic and acoustic methods for characterization of steel sheets materials*. Steel and Iron, (2000),No.12, p 115-121
8. Hellier, C.J.,: *Handbook of nondestructive evaluation*, New York, McGraw-Hill, 2003
9. Janousek, L., Smetana,M., and Capova,K.,: *Enhancing information level in eddy-current non-destructive inspection*, Intl. J. Appl. Electr.Mech., (2010),No.33, p 1149-1155
10. J.G.,Martin, Gil,J.G., and Sanchez,E.V.,: *Non-destructive techniques based on Eddy current testing*, Sensors, (2011), No.11, p 2525-2565
11. Shull,P.J.,: *Nondestructive evaluation: Theory, techniques and applications*, CRC Press, 2002.
12. Calvano,F.,: *Electromagnetic nondestructive evaluation and inverse problems*, PhD thesis, departement of electrical engineering, Napoli university, 2010
13. Bossavit, A., and Verite,J.C.,: *A Mixed FEM-BIEM method to solve 3-D eddy current problems*, IEEE Trans. on Magn.,(1982),No.18,p 431-435
14. Carpenter,C.J.,: *Comparison of alternative formulations of 3-D magnetic field and eddy current problem at power frequencies*, IEE Proc.,(1977),No.124,p 1026-1034.
15. Brown,N.L.,: *Calculation of 3-D eddy currents at power frequencies*, IEE Proc., (1982), No.129, p 46-53.
16. Albanese,R., Rubinacci,G.,: *Solution of three dimensional eddy current problems by integral and differential methods*, IEEE Trans. Magn., (1988), No.24, p 98-101.
17. Biro,O., and Preis,K.,: *On the Use of the magnetic vector potential in the finite element analysis of three-dimensional eddy currents*, IEEE Trans. Magn.,(1989), No.25, p 3145-3159
18. Ribeiro,A., Ramos,H., and Gonçalves,J.,: *Lift-off insensitive thickness measurement of aluminum plates using harmonic eddy current excitation and a GMR sensor*, Measurement, (2012), No.45, p 2246-2253.
19. Xu,Z., Wu,X., Li,J., and Kang,Y.,: *Assessment of wall thinning in insulated ferromagnetic pipes using the time-to-peak of differential pulsed eddy- current testing signals*, NDT & E. International,(2012), No.51, p 24-29.
20. Rubinacci,G., Tamburino,A., and Ventre,S.,: *Fast numerical techniques for electromagnetic nondestructive evaluation*, NDT & E. International, (2009), No.24, p 165-194.
21. Ribeiro,A.L., Ramos,H.G., and Postolache,O.,: *A simple forward direct problem solver for eddy current non-destructive inspection of aluminum plates using uniform field probes*, Measurement, (2011), No.45, p 213-217.
22. Bakhtiari,S., and Kupperman,D.S.,: *Modeling of eddy current probe response for steam generator tubes*, Nuclear Engineering and Design,(1999), No. 194, p 57-71.
23. Bennoud,S., Zergoug,M., and Allali,A.,: *Numerical simulation for cracks detection using the finite elements method*, Int. journal of multiphysics, (2014), No.8, p 1-10.
24. Simm, A., Theodoulidis, T., Poulakis, N., Tian, G.Y.,: *Investigation of the magnetic field response from eddy current inspection of defects*, Int J Adv Manuf Technol (2011), No.54, p 223-230
25. Xie,S., Chen,Z., Takagi, T., Uchimoto,T.,: *Efficient numerical solver for simulation of pulsed eddy current testing signals*, IEEE Trans. Magn., (2011), No. 47, p 4582-4591.
26. Stott,C.A., Underhill,P.R., Babbar,V.K., and Krause,T.W.,: *Pulsed eddy current detection of cracks in multilayer aluminum lap joints*, IEEE Sensors J., (2015), No. 2, p 956-962
27. Glorieux,C., Moulder,J. Basart, J., and Thoen,J.,: *The determination of electrical conductivity profiles using neural network inversion of multi-frequency eddy-current data*, J. Phys. D: Appl. Phys., (1999), No.32, p 616-622.
28. Ravan,M., Sadeghi, S.H.H., and Moini,R.,: *Neural network approach for determination of Fatigue crack depth profile in a metal, using alternating current field measurement data*, IET Sci., Meas.Tech., (2008), No.2 p 32-38.
29. Chady,T., Enokizono, M., and Sikora,R.,: *Neural network models of eddy current multi-frequency system for nondestructive testing*, IEEE Trans. on Magn., (2000), No.36, p 1724-1727
30. Rosado,L.S., Janeiro,F.M., Ramos,P.M., and Piedade,M.,: *Defect characterization with eddy current testing using nonlinear-regression feature extraction and artificial neural networks*, IEEE Trans. Instr. Meas., (2013), No.62, p 1207-1244.
31. Xie,S., Chen,Z., Wang,L., Takagi,T., Uchimoto,T.: *An inversion scheme for sizing of wall thinning defects from pulsed eddy current testing signals*, Int. J. Appl. Electromagn.Mech.,(2012), No.32, p 203-211.